

Short Communication

Synthesized N1, N2-bis (furan-2-ylmethylene)Benzene-1, 2-diamine as a Corrosion Inhibitor for 20# Carbon Steel in 1 M Hydrochloric Acid

Zuoan Xiao^{1,2}, Huawei Wu¹, Guijie Liang³, Dan Zhan^{2,*}

¹ Hubei Key Laboratory of Power System Design and Test for Electrical Vehicle, Xiangyang 441053, P. R. China

² Department of Chemical Engineering and Food Science, Hubei University of Arts and Science, Xiangyang, 441053, P. R. China

³ Hubei Key Laboratory of Low Dimensional Optoelectronic Materials and Devices, Xiangyang, 441053, P. R. China

*E-mail: dan_zhan@126.com

Received: 19 July 2017 / Accepted: 5 September 2017 / Published: 12 October 2017

N1, N2-Bis (furan-2-ylmethylene) benzene-1,2-diamine (SB) was synthesized and investigated as a 20# carbon steel inhibitor in 1 M hydrochloric acid. Electrochemical and weight loss (WL) measurements were employed for evaluating the inhibition properties of SB. It was shown that SB acted as a mix-type corrosion inhibitor during the process, and the charge transfer resistance increased, while the double layer capacitance decreased with the increasing SB concentration. The results implied that the inhibiting effect of SB was attributed to the covering layer formed on the steel surface that replaced the water molecule. The thermodynamic adsorption parameters obtained from the WL measurements demonstrated that the adsorption process is exothermic and spontaneous, and the adsorption of SB obeys a Langmuir adsorption isotherm. The calculated values of $\Delta G_{\text{ads}}^{\circ}$ revealed that the adsorption mechanism of SB on the steel surface is a combination of physical and chemical processes.

Keywords: furfural; o-diaminobenzene; corrosion inhibitor; adsorption

1. INTRODUCTION

As a constructional material, carbon steel is used extensively in many industries due to its stiffness and high strength-to-weight ratios. It is susceptible to attack when exposed to an aggressive medium, such as industrial cleaning, acid derusting and petrochemical industry [1-3]. Therefore, the corrosion protection of carbon steel in corrosive medium has attracted considerable interest. Several

approaches are used to prevent metals from corroding, such as anodic or cathodic protection, coatings, oxidizing or phosphating treatments and corrosion inhibitors [4]. Among them, the use of corrosion inhibitors is considered to be the most convenient and cost-effective method for aqueous acidic corrosive media.

Corrosion inhibitors can slow down the reaction between metals and aggressive media when added at proper concentrations. In recent years, many inhibitors have been investigated for exploring the relationship between inhibition efficiency and the molecular structure of the inhibitor [5, 6]. Many researchers [7, 8] have reported that organic compounds containing multiple bonds as well as aromatic rings and/or heteroatoms (such as N, O, S) generally exhibit good inhibitive properties. Schiff bases are organic compounds derived from the condensation reaction between aldehydes and amine, and they have been applied effectively against the corrosion of steel [5, 9-11], aluminum [12, 13], copper [14-16], magnesium [17] and other alloy materials [18, 19] in acidic environments. The effective corrosion inhibition properties originated from the presence of double bonds and heteroatoms in the molecules. Moreover, numerous Schiff bases can be synthesized easily using relatively cheap aldehydes and amines.

In the present work, a Schiff base named N1, N2-bis (furan-2-ylmethylene) benzene-1, 2-diamine was synthesized, which consists of an aromatic ring, double bonds and heteroatoms. This chemical structure (as shown in Fig. 1) provides a scientific theoretical foundation for corrosion inhibition properties. The inhibition performance of SB on 20# carbon steel in 1 M hydrochloric acid was evaluated using electrochemical and weight loss measurements. The adsorption mechanism of SB on the carbon steel surface was explored in detail.

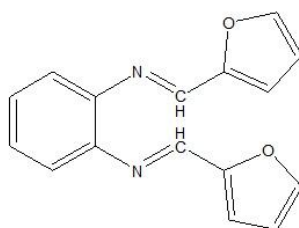


Figure 1. Chemical structure of N1, N2-bis (furan-2-ylmethylene) benzene-1,2-diamine (SB)

2. EXPERIMENTAL

2.1 Synthesis of the Schiff base

The furfuraldehyde was purified through vacuum distillation before use, and the other reagents were used without any pretreatment. First, the ethanolic solution of furfuraldehyde (4 mmol) was added to an ethanolic solution of *o*-phenylenediamine (2 mmol) and then refluxed with stirring for 4 h at room temperature. The obtained deep red oily product was taken out and stored at room temperature until the solvent was completely volatilized. A light-yellow product was obtained after dissolving and

purifying the product through hot cyclohexane. The Schiff base (SB) was added to the 1 M hydrochloric acid at concentrations of 0.04 g L⁻¹, 0.2 g L⁻¹, 1 g L⁻¹, and 5 g L⁻¹.

2.2 Electrochemical method

Working electrodes were prepared using a 20# carbon steel sheet (diameter=0.8 cm) with a composition (wt %) of C 0.17~0.23, Mn 0.35~0.65, Si 0.17~0.37, S≤0.035, P≤0.035, Ni≤0.30, Cr≤0.15, Cu≤0.25, and Fe (balance). The 20# carbon steel sheets were embedded in epoxy resin. Then, the samples were polished to a mirror finish using abrasive paper (grade 200-400-800-1200-2000) in order to gain the exposed and flat surface of the electrode. Finally, the working electrodes were degreased with acetone, and dried under warm air flow.

The electrochemical measurements were conducted using a CHI 660A Electrochemical Workstation (Chenhua, China) in a three-electrode cell at (20±1) °C, a platinum foil was employed as the counter electrode and a saturated calomel electrode (SCE) as the reference electrode. Before each electrochemical measurements, the samples were placed in 1 M hydrochloric acid for 30 minutes to record the open circuit potential (OCP). All the chemicals were of analytic grade.

The potentiodynamic polarization measurements were carried out in the potential between -900 and -200 mV vs. SCE with a scanning rate of 0.5 mV S⁻¹ at 20 °C. The values of inhibition efficiency (*IE* %) and surface coverage (*θ*) were calculated according to equations (1) and (2), respectively [20, 21]. Where *i*_{corr}⁰ and *i*_{corr} are the corrosion current densities of the 20# carbon steel without and with the inhibitor in 1 M hydrochloric acid, respectively.

$$IE\% = \frac{i_{corr}^0 - i_{corr}}{i_{corr}^0} \times 100 \quad (1)$$

$$\theta = \frac{i_{corr}^0 - i_{corr}}{i_{corr}^0} \quad (2)$$

Electrochemical impedance spectroscopy (EIS) experiments were performed in a frequency range from 10⁵ to 10⁻² Hz with an amplitude of 10 mV peak-to-peak using AC signals at the OCP. Each impedance data was analyzed with the software “ZViewII”. The *IE*% of the used inhibitors obtained from EIS was calculated by applying the following relation [22], where *R*'_{ct} and *R*_{ct} are the charge transfer resistances in the presence and absence of the inhibitor, respectively.

$$IE\% = \frac{R_{ct}' - R_{ct}}{R_{ct}'} \times 100 \quad (3)$$

2.3 Weight loss measurements

The 20# carbon steels with rectangular forms (35×10×1.5 mm) were weighed using an electronic balance, and then suspended in a 1 M hydrochloric acid containing SB with different concentrations in a thermostatic bath; the samples were immersed for 3 h at 293, 303, 313 and 323 K, respectively. After that, the surfaces of the specimens were cleaned using double distilled water (the

corrosion products, if present, were removed), rinsed by acetone, dried, and then weighed again. To ensure good reproducibility, experiments were made in triplicate. The values of the corrosion rate (CR), θ , and $IE\%$ were calculated according to the following equation [23, 24], where ΔW means the average weight loss of three specimens (mg), s means the surface area of one specimen (cm^2), t means the immersion time (h), and CR_0 and CR ($mg\ cm^{-2}\ h^{-1}$) are the corrosion rates of the 20# carbon steel in the 1 M hydrochloric acid with and without SB, respectively.

$$CR = \frac{\Delta W}{st} \quad (4)$$

$$IE\% = \frac{CR_0 - CR}{CR_0} \times 100 = \theta \times 100 \quad (5)$$

3. RESULTS AND DISCUSSION

3.1 Potentiodynamic polarization measurements

The polarization diagram for the corrosion of 20# carbon steel in the 1.0 M hydrochloric acid solution containing inhibitors with different concentrations are presented in Fig. 2. The corrosion parameters like corrosion current density (i_{corr}), corrosion potential (E_{corr}), anodic and cathodic Tafel slopes (β_a, β_c), surface coverage and corrosion inhibitor efficiency are calculated and demonstrated in Table 1. It is evident that both the cathodic and anodic current dropped with the addition of SB in the acidic environment, implying that SB was a mixed-type inhibitor and could reduce the anodic dissolution and suppress the cathodic hydrogen evolution via covering the surface active sites on carbon steel [2, 3, 25]. It was previously reported that, if the displacement in E_{corr} is more than ± 85 mV relative to the E_{corr} of the blank, the inhibitor can be regarded as a cathodic- or anodic-type inhibitor [26]. As could be seen from Table 1, the maximum displacement in E_{corr} is 39 mV, indicating that SB is a mixed-type corrosion inhibitor. The E_{corr} values shifted slightly toward the positive direction, suggesting that the adsorption of SB on the steel had a prevailing effect at the anodic site. Additionally, the slight shift in E_{corr} indicates that the inhibition probably resulted from a geometric blocking effect of the inhibitive species adsorbed on the surface of the corroding metal [27]. It is evident that the inhibition efficiency increased while the i_{corr} values decreased as the concentration of SB increased. This result discloses that SB acts by adsorbing on the metal surface to form a protective film. Moreover, the values of the anodic and cathodic Tafel slopes changed slightly with various concentrations of SB, showing that SB interfered with both the cathodic and the anodic reactions. This result provided further evidence that the behavior of SB was mixed.

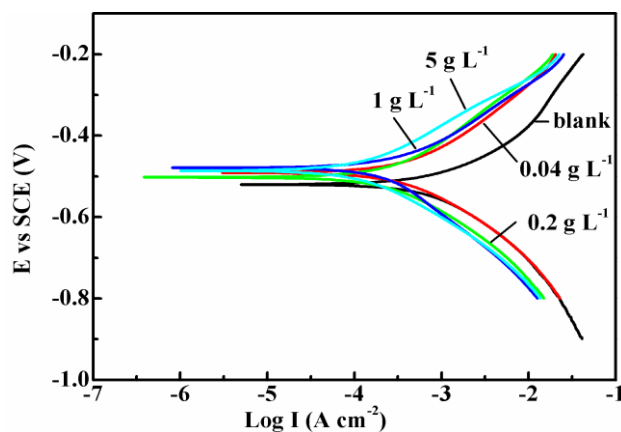


Figure 2. Potentiodynamic polarization curves for the 20# carbon steel in 1.0 M hydrochloric acid without and with different concentrations of SB

Table 1. Electrochemical polarization parameters for the 20# carbon steel in 1 M hydrochloric acid without and with different concentrations of SB

C (g/L)	$-E_{corr}/mV$	$10^6 i_{corr}/(A.cm^2)$	$\beta a (mV/dec)$	$-\beta c(mV/dec)$	θ	IE%
0	527.0	1638.0	96	103		
0.04	494.0	748.6	98	101	0.5430	54.30
0.2	505.0	526.4	87	97	0.6786	67.86
1	492.6	510.2	82	86	0.6891	68.91
5	488.7	268.4	75	79	0.8361	83.61

3.2 Electrochemical impedance spectroscopy

The electrochemical impedance was applied to assess the inhibition property of SB. The influence of SB concentration on the impedance behavior of the 20# carbon steel is displayed in Fig. 3. It is obvious that the shapes of all plots are similar, and the semicircle radii in these plots vary significantly. The shape was maintained after the addition of SB, indicating that the mechanism of steel dissolution did not change in contrast to the blank solution. The semicircle radii of the Nyquist plot increased with the increasing concentration of SB. This implies that a protective layer formed after SB adsorbed on the steel surface.

It should be noted that the Nyquist plots display a single slightly depressed capacitive semicircle, indicating that the dissolution process at the electrode/solution interface was controlled by charge transfer reactions. Meanwhile, the depression of Nyquist semicircles, as mentioned in previous literature [28, 29], is generally ascribed to the roughness, impurities, dislocations of metal surfaces.

The electrical equivalent circuit is presented in the inset of Fig. 3, where R_s means the solution resistance, C_{dl} means the double layer capacitance and R_{ct} means the charge transfer resistance. The resistor R_s is in series with the C_{dl} and R_{ct} , while C_{dl} is in parallel with the R_{ct} . The electrochemical

parameters, such as R_s , C_{dl} , R_{ct} and $IE\%$ calculated from EIS are displayed in Table 2. It is obvious that R_{ct} values increased with the addition of SB, and this effect was reinforced with the increase in SB concentration.

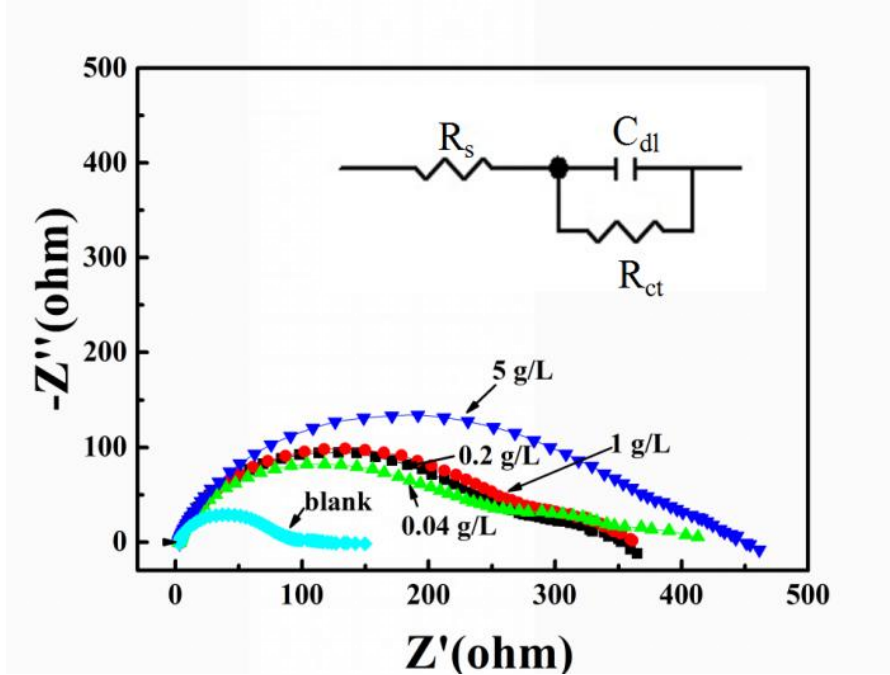


Figure 3. Nyquist plots for 20# carbon steel in 1.0 M hydrochloric acid containing SB with different concentrations. The inset shows the electrical equivalent circuit diagram for EIS experimental

Table 2. Electrochemical impedance spectroscopy results for 20# carbon steel in 1 M hydrochloric acid containing SB with various concentrations

C (g/L)	R_s	$10^5 C_{dl}/F.cm^{-2}$	$R_{ct}/\Omega.cm^{-2}$	θ	$IE\%$
0	6.56	10.25	132.76		
0.04	7.31	9.05	344.4	0.6145	61.45
0.2	7.79	8.09	399.2	0.6674	66.74
1	7.22	6.03	400.4	0.6684	66.84
5	7.20	7.53	526.4	0.7478	74.78

The results reveal that SB molecules adsorbed on the carbon steel, and the coverage of the metal surface increased with the increasing SB concentration. In contrast, the C_{dl} values decreased, which was ascribed to the drop in the local dielectric constant and/or a rise in the thickness of the electrical double layer. The results prove that SB molecules functioned by forming a protective layer through gradually replacing water molecules on the 20# carbon steel surface[23]. This protective layer reduced the active surface area of the carbon steel and suppressed the anodic reaction in 1 M hydrochloric acid.

From Tables 1 and 2, SB can decrease the corrosion rate of carbon steel at increased concentrations in 1 M hydrochloric acid, however, the *IE* % of SB is inferior to that of other Schiff bases [3, 25]. It is well known that the *IE* % is closely related to the adsorption of inhibition molecules. As seen from Fig. 1, SB should be a good inhibitor that can interact with the metal surface due to its aromatic rings (π -electron) and heteroatoms (N, O). However, it is obvious that the degree of surface coverage was low, from Tables 1 and 2. We believe that steric hindrance is one of the crucial factors that affected the interaction between SB and carbon steel surface.

3.3 Weight loss measurements

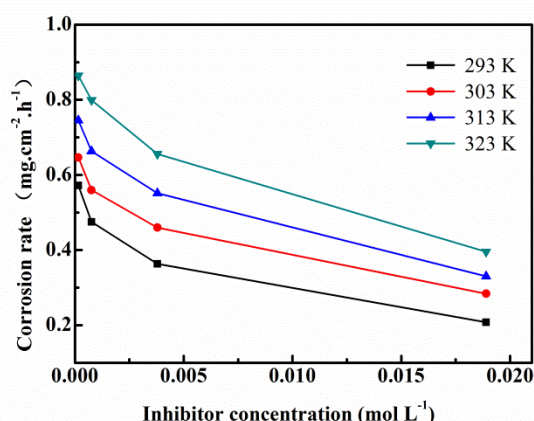


Figure 4. Plots of the corrosion rate against SB concentration for the 20# carbon steel in 1 M hydrochloric acid for weight loss measurements at different temperatures

Table 3. Calculated corrosion parameters for the 20# carbon steel in 1 M hydrochloric acid without and with various concentrations of SB for weight loss measurements at different temperatures

<i>C</i> (g/L)	<i>CR</i> (mg.cm ⁻² .h ⁻¹)				θ				<i>IE</i> %			
	293K	303K	313K	323K	293K	303K	313K	323K	293K	303K	313K	323K
0.00	1.5748	1.6947	1.8032	1.9741								
0.04	0.5721	0.6469	0.7352	0.8643	0.6367	0.6183	0.5923	0.5549	63.67	61.83	59.23	55.49
0.20	0.4750	0.5598	0.6634	0.7992	0.6984	0.6697	0.6321	0.5884	69.84	66.97	63.21	58.84
1.00	0.3633	0.4599	0.5514	0.6557	0.7693	0.7286	0.6942	0.6623	76.93	72.86	69.42	66.23
5.00	0.2077	0.2839	0.3302	0.3953	0.8681	0.8325	0.8169	0.7964	86.81	83.25	81.69	79.64

Figure 4 shows the corrosion rate (*CR*) against SB concentration plots of 20# carbon steel in the 1 M hydrochloric acid at different temperatures. It is obvious that the *CR* of 20# carbon steel in the acid corrosive environment decreased with the increase of SB concentration at all the studied temperatures. It can also be found that the *CR* increased more rapidly with the increased temperature in both the inhibited and uninhibited solutions. This indicates that the adsorption process of SB reduced the number of active sites on the metal surface. Therefore, the adsorption process became weakened with the increase in the temperature. It is well known that the adsorption and desorption processes took

place in opposite directions simultaneously at equilibrium. Multifarious factors, such as the concentration of inhibitor and the temperature of corrosive media, shifted the direction of the equilibrium. At higher temperatures, more of SB desorbed from the metal/solution interface which lead to increased corrosion rate and poor inhibition performance.

The values of CR, θ and $IE\%$ calculated from WL measurements are shown in Table 3. It can be observed that CR obviously decreased when the inhibitor was added at all temperatures. This result displayed that SB is an effective inhibitor for 20# carbon steel in 1 M hydrochloric acid. Meanwhile, it was also noted that θ and $IE\%$ increased with the increased concentration and decreased temperature. The results are consistent with the abovementioned results of the electrochemical measurements.

3.4 Adsorption isotherm

Generally speaking, it is considered that inhibitor molecules establish their inhibition action through adsorbing onto the metal surface. Therefore, adsorption isotherms can be investigated to explore degree of interaction between the inhibitor and metal surface in the corrosive system. To obtain detailed information about adsorption process, experimental data obtained from WL measurements were tried to fit several isotherms like Langmuir, Freundlich, Temkin, Frumkin and Flory-Huggins isotherms. It is found that the correlation coefficients of the Langmuir adsorption isotherm vary between 0.9990 and 0.9996 for all temperatures, the results show that the adsorption of SB on the 20# carbon steel surface obeys Langmuir adsorption isotherm. Such isotherms suggest that each adsorbed molecule remains in one active site on the metal surface and the adsorbed species do not interact with each other [30]. Langmuir adsorption is shown according to the following equation (6),

$$\frac{C}{\theta} = \frac{1}{K_{ads}} + C \quad (6)$$

where C is the molar concentration of SB, K_{ads} is the equilibrium constant of adsorption-desorption process, and θ was calculated from WL experimental results using Equation 5. The values of C/θ against the SB concentration (C) between 293 K and 323 K are displayed in Fig. 5. The K_{ads} values were calculated from the intercept of the plotted lines in Fig. 5.

The thermodynamic parameters of the adsorption process, such as the standard free energy (ΔG^o_{ads}), enthalpy (ΔH^o_{ads}) and entropy (ΔS^o_{ads}), were calculated using the following equations, respectively[24]:

$$K_{ads} = \frac{1}{55.5} \exp\left(-\frac{\Delta G^o_{ads}}{RT}\right) \quad (7)$$

$$\ln K_{ads} = -\frac{\Delta H^o_{ads}}{RT} + \text{constant} \quad (8)$$

$$\Delta G^o_{ads} = \Delta H^o_{ads} - T\Delta S^o_{ads} \quad (9)$$

where R is the gas constant and T is the absolute temperature. Fig. 6 shows the plots of $\ln K_{ads}$ versus $1/T$ in 1 M hydrochloric acid containing various SB concentrations for 20# carbon steel. The value of ΔH^o_{ads} was obtained from the slope of plotted straight line.

All the thermodynamic parameters obtained from the data of WL measurements are displayed in Table 4. As observed, the K_{ads} values decreased with the increasing temperature, suggesting that SB molecules were physically adsorbed on the surface of carbon steel, and the adsorption ability of SB on the carbon steel surface weakened with the increasing temperature. Furthermore, the relatively higher negative value of ΔG^o_{ads} indicated that the adsorption was a spontaneous process, and strong inhibition interactions occurred with the 20# carbon steel surface in the 1 M hydrochloric acid. It is widely accepted that ΔG^o_{ads} values near or higher than -20 kJ mol^{-1} indicate physisorption, and these adsorption processes are associated with electrostatic interactions between charged molecules and charged metal surfaces[31]. For ΔG^o_{ads} values near -40 kJ mol^{-1} , the type of adsorption can be considered as chemisorption, which involves charge sharing or transfer from organic molecules to metal surfaces to form a coordinate-type of metal bond during the process[4, 31]. The data of ΔG^o_{ads} presented in Table 4 are in the range of -29.75 to $-31.46 \text{ kJ mol}^{-1}$. The ΔG^o_{ads} values are between the threshold values for physical adsorption and chemical adsorption, indicating that the adsorption of SB on the 20# carbon steel surface is a mixed type of physical and chemical adsorption.

The adsorption enthalpy is also a valuable tool for understanding the adsorption behavior of an inhibitor. For $\Delta H^o_{ads} > 0$, the positive heat of adsorption is ascribed explicitly to chemisorption, and for $\Delta H^o_{ads} < 0$, the negative heat of adsorption may be concerned with either physisorption or chemisorption and/or a mixture of both process[32]. The ΔH^o_{ads} values from the weight loss measurements are negative which indicated that the adsorption process is somewhat unfavorable at elevated temperatures. In another words, the corrosion inhibition efficiency declined with the temperature rise. In an exothermic process, physisorption is easily distinguished from chemisorption according to the absolute value of ΔH^o_{ads} . If the absolute value is lower than $41.86 \text{ kJ mol}^{-1}$, a physisorption mechanism or mixture of physisorption and chemisorption mechanism operates, while for values close to 100 kJ mol^{-1} , a chemisorption mechanism acts[30]. The calculated values of ΔH^o_{ads} is $-13.36 \text{ kJ mol}^{-1}$, suggesting that the adsorption of SB on the carbon steel surface can be considered as a physisorption or a mixture of a physisorption and chemisorption.

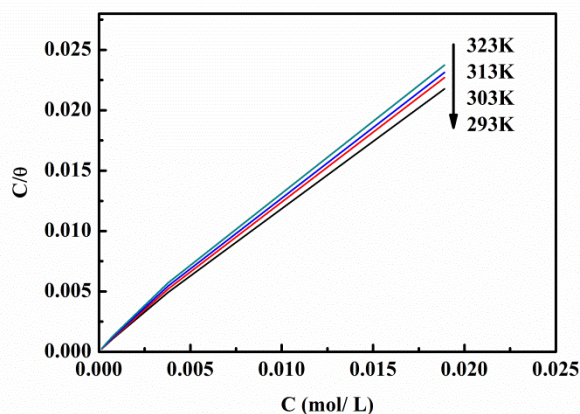


Figure 5. The corrosion data used to fit Langmuir isotherm adsorption for 20# carbon steel in 1 M hydrochloric acid at different temperatures

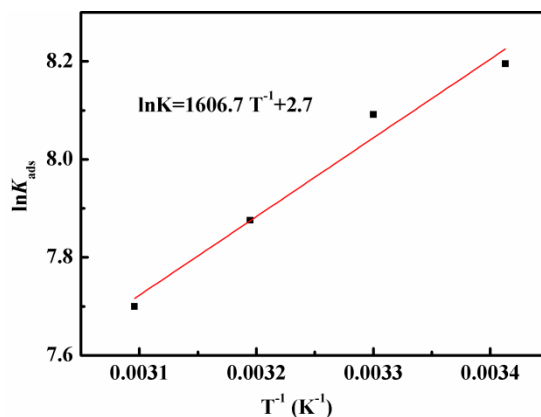


Figure 6. $\ln K_{ads}$ against $1/T$ curves in 1 M hydrochloric acid containing different concentrations of SB for 20# carbon steel

Table 4. Adsorption thermodynamic parameters of SB on 20# carbon steel surface in 1 M hydrochloric acid at different temperatures

Temperature(K)	R^2	$K_{ads} (L mol^{-1})$	$\Delta G^o_{ads} (KJ mol^{-1})$	$\Delta H^o_{ads} (KJ mol^{-1})$	$\Delta S^o_{ads} (J K^{-1} mol^{-1})$
293	0.9992	3623.66	-29.7475	-13.3581	55.9337
303	0.9990	3265.91	-30.5010	-13.3581	56.5772
313	0.9984	2632.13	-30.9226	-13.3581	56.1166
323	0.9980	2206.74	-31.4615	-13.3581	56.0477

Based on the results obtained from the values of ΔG^o_{ads} , it can be concluded that the adsorption mechanism is combined physisorption with chemisorption existing between SB and carbon steel surface. From the table 4, the positive sign of ΔS^o_{ads} means an increase in disorder in the system, which was attributed to more water molecules being replaced by inhibitor molecules.

4. CONCLUSIONS

The inhibition effect of SB as an inhibitor of 20# carbon steel in 1 M hydrochloric acid was evaluated through electrochemical and weight loss measurements. Based on the results of above mentioned study, conclusions were drawn as follow:

- 1) SB is an effective inhibitor, and it acts as a mixed-type inhibitor for 20# carbon steel in 1 M hydrochloric acid, which inhibits the corrosion of carbon steel by blocking the active sites of the metal surface.
- 2) The impedance curves indicated that the R_{ct} values rised, while the C_{dl} values dropped with the increasing concentration of inhibitor.
- 3) The inhibition efficiency increased with the increasing SB concentration and decreased with an increase in the temperature.

4) The IE % obtained from the weight loss experiments had the same variation trend as that obtained from potentiodynamic polarization and electrochemical impedance spectroscopy measurements.

5) The adsorption of SB on the 20# carbon steel obeys the Langmuir adsorption isotherm. The negative value of ΔG°_{ads} indicates that SB was adsorbed on the surface of carbon steel, and this adsorption was a spontaneous process.

6) The calculated ΔG°_{ads} values are in the range of -29.75 to -31.46 kJ mol^{-1} , revealing that the adsorption process is a cooperation phenomenon between physisorption and chemisorption.

ACKNOWLEDGEMENTS

This work was supported by National Science Foundation of China (51708191), the open funds of Hubei Key Laboratory of Power System Design and Test for Electrical Vehicle (HBUASEV2017F009, 10), the Project for Discipline Groups Construction of Food New-type Industrialization of Hubei University of Arts and Science, and the project for Discipline Group with Advantages and Characteristic of Electromechanics & automobile of Hubei Province (XKQ2017021, 022).

References

1. M.A. Hegazy, I. Aiad, *J. Indu. Eng. Chem.*, 31(2015) 9.
2. A. Biswas, S. Pal, G. Udayabhanu, *Appl. Surf. Sci.*, 353 (2015) 173.
3. B. M. Mistry, S. Jauhari, *Res. Chem. Intermed.*, 41 (2014) 1.
4. N. A. Negm, F. M. Ghuiba, S. M. Tawfik, *Corr. Sci.*, 53 (2011) 3566.
5. A.I. Adawy, M. A. Abbas, K. Zakaria, *Res. Chem. Intermed.*, 42 (2016) 3385.
6. N. Soltani, H. Salavati, N. Rasouli, M. Pazireh, A. Moghadasi, *Chem. Eng. Comm.*, 203 (2016) 840.
7. I. Belfilali, A. Chetouani, B. Hammouti, S. Louhibi, A. Aouniti, S.S. *Res. Chem. Intermed.*, 40 (2014) 1069.
8. M. Athar, H. Ali, M. A. Quraishi, *Bri. Corr. J.*, 37 (2013) 155.
9. I. A. Aiad, N. A. Negm, *J.Surf. Deter.*, 12 (2009) 313.
10. N. K. Bakirhan, A. Asan, N. Colak, S. Sanli, *J. Chil. Chem. Soc.*, 61 (2016) 3066.
11. S. K. Saha, A. Dutta, P. Ghosh, D. Sukul, P. Banerjee, *Phys. Chem. Chem. Phys.*, 17 (2015) 5679.
12. H. Ashassi-Sorkhabi, B. Shabani, B. Aligholipour, D. Seifzadeh, *Appl. Surf. Sci.*, 252 (2006) 4039.
13. N.A. Negm, M.F. Zaki, *Coll. Surf. A*, 322 (2008) 97.
14. A. Dadgarinezhad, F. Baghaei, *G. Uni. J. Sci.*, 23 (2010) 287.
15. F. B. Ravari, A. Dadgarinezhad, I. Shekhshoei, *G. Uni. J. Sci.*, 22 (2009) 175.
16. J. Zhang, Z. Liu, G. C. Han, S. L. Chen, Z. Chen, *Appl. Surf. Sci.*, 389 (2016) 601.
17. D. Seifzadeh, A. Bezaatpour, A. N. Shamkhali, H. Basharnavaz, *Trans. Indian. Ins. Meta.*, 69 (2016) 1.
18. A. Aytaç, Ü. Özmen, M. Kabasakaloğlu, *Mater. Chem. Phys.*, 89 (2005) 176.
19. S. Thirugnanaselvi, S. Kuttirani, A.R. Emelda, *Trans. Nonfer. Meta. Soc.*, 24 (2014) 1969.
20. M.G. Hosseini, H. Khalilpur, S. Ershad, L. Saghatforoush, *J. Appl. Electrochem.*, 40 (2010) 215.
21. A. S. Fouda, H. A. Mostafa, H. M. El-Abbasy, *J.Appl. Electrochem.*, 40 (2010) 163.
22. M. Shabani-Nooshabadi, M.S. Ghandchi, *J. Indu. Eng. Chem.*, 31 (2015) 231.
23. A. S. Fouda, K. Shalabi, A. A. Idress, *Green Chem. Lett. Rev.*, 8 (2015) 17.
24. T. M. Lv, S. H. Zhu, L. Guo, S. T. Zhang, *Res. Chem. Intermed.*, (2014) 1.
25. M. Farsak, H. Keleş, M. Keleş, *Corr. Sci.*, 98 (2015) 223.

26. I. Ahamad, C. Gupta, R. Prasad, M. A. Quraishi, *J. Appl. Electrochem.*, 40 (2010) 2171.
27. C. Cao, *Corr. Sci.*, 38 (1996) 2073.
28. R. S. Erami, M. Amirnasr, K. Raeissi, M. M. Momeni, S. Meghdadi, *J. Ira. Chem.Soc.*, 12 (2015) 1.
29. K. R. Ansari, M. A. Quraishi, *J. Taiwan Ins. Chem. Eng.*, 54 (2015) 145.
30. G. Avci, *Coll.Surf. A*, 317 (2008) 730.
31. R. Solmaz, E. Altunbaş, G. Kardaş, *Mater. Chem. Phys.*, 125 (2011) 796.
32. S. H. Zaferani, M. Sharifi, D. Zaarei, M. R. Shishesaz, *J. Envir. Chem.Eng.*, 1 (2013) 652.

© 2017 The Authors. Published by ESG (www.electrochemsci.org). This article is an open access article distributed under the terms and conditions of the Creative Commons Attribution license (<http://creativecommons.org/licenses/by/4.0/>).